Science Signaling
AAAS

www.sciencesignaling.org/cgi/content/full/9/423/ra38/DC1

Supplementary Materials for

Gβ promotes pheromone receptor polarization and yeast chemotropism by inhibiting receptor phosphorylation

Amber Ismael, Wei Tian, Nicholas Waszczak, Xin Wang, Youfang Cao, Dmitry Suchkov, Eli Bar, Metodi V. Metodiev, Jie Liang, Robert A. Arkowitz, David E. Stone*

*Corresponding author. E-mail: dstone@uic.edu

Published 12 April 2016, *Sci*. *Signal*. **9**, ra38 (2016)
DOI: 10.1126/scisignal.aad4376

The PDF file includes:

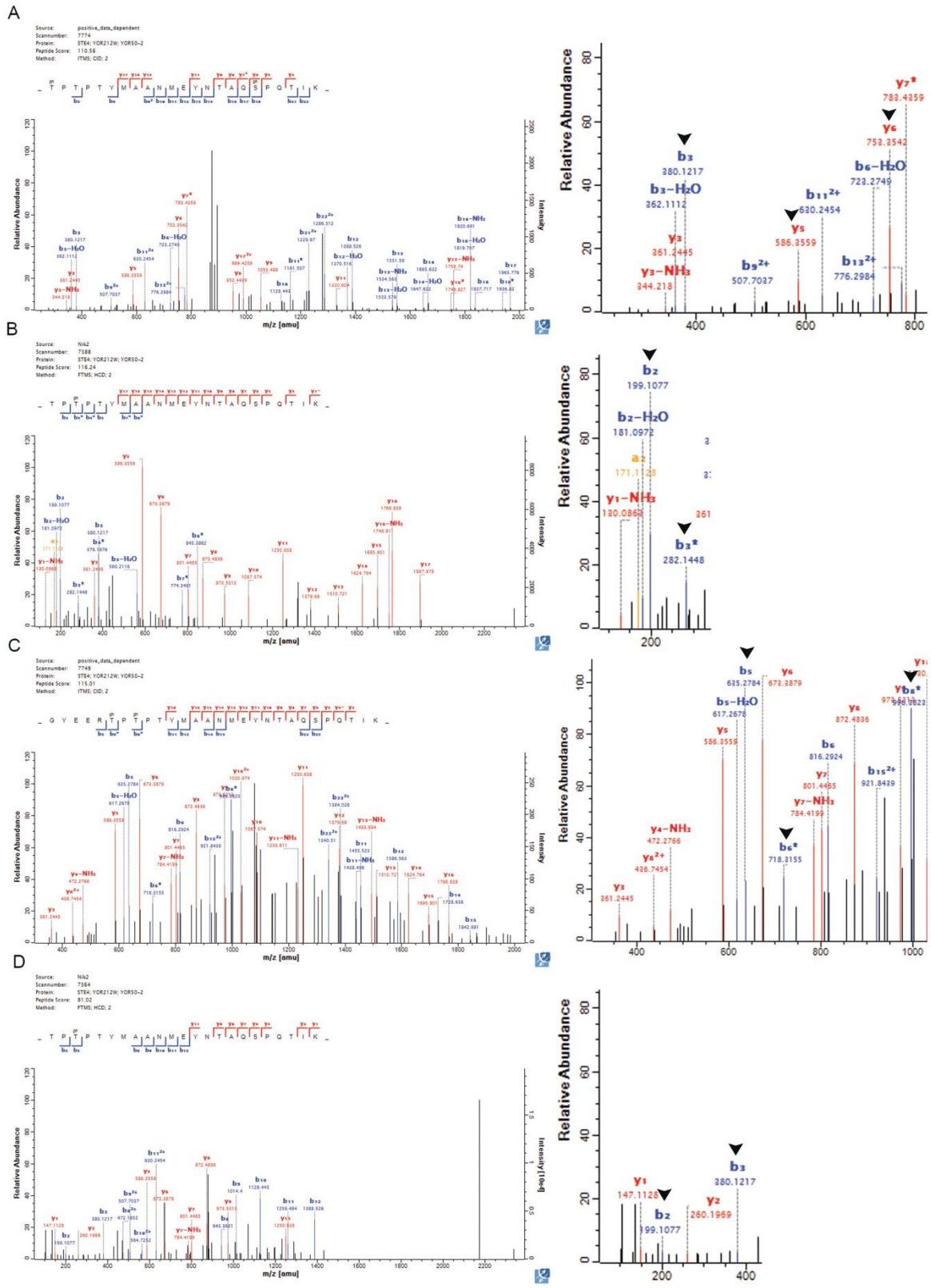

(Fig. S1)

Fig. S1. Examples of mass spectra used to map the sites of pheromone-induced Gβ phosphorylation. (**A** to **D**) Samples prepared from vegetative cells overexpressing Gβγ in normal medium and pheromone-treated cells overexpressing Gβγ in heavy medium were analyzed together by mass spectrometry to identify sites of pheromone-induced phosphorylation of Gβ. The diagnostic fragment ions are indicated by arrowheads. (A) Collision-induced dissociation (CID) spectrum of a doubly phosphorylated peptide locating the phosphates at Ser^{335} and either of Thr^{318} or Thr^{320}. The diagnostic fragment ions for Ser^{335} are y_5 and y_6, whereas that for Ser^{318}/Ser^{320} is b_3. The Andromeda score is 110. (B) High-resolution, high-collision energy dissociation spectrum (HCD) of the singly phosphorylated peptide locating the phosphate at Thr^{320}. The diagnostic ions are b_2 and b_3. The Andromeda score is 116. (C) CID spectrum of a doubly phosphorylated peptide locating the phosphates at Thr^{318} and Thr^{320}. The diagnostic fragment ions are b_5, b_6, and b_8. The Andromeda score is 115. (D) HCD spectrum of the singly phosphorylated peptide locating the phosphate at Thr^{320}. The diagnostic fragment ions are b_2 and b_3. The Andromeda score is 81. Spectra are representative of two independent experiments.

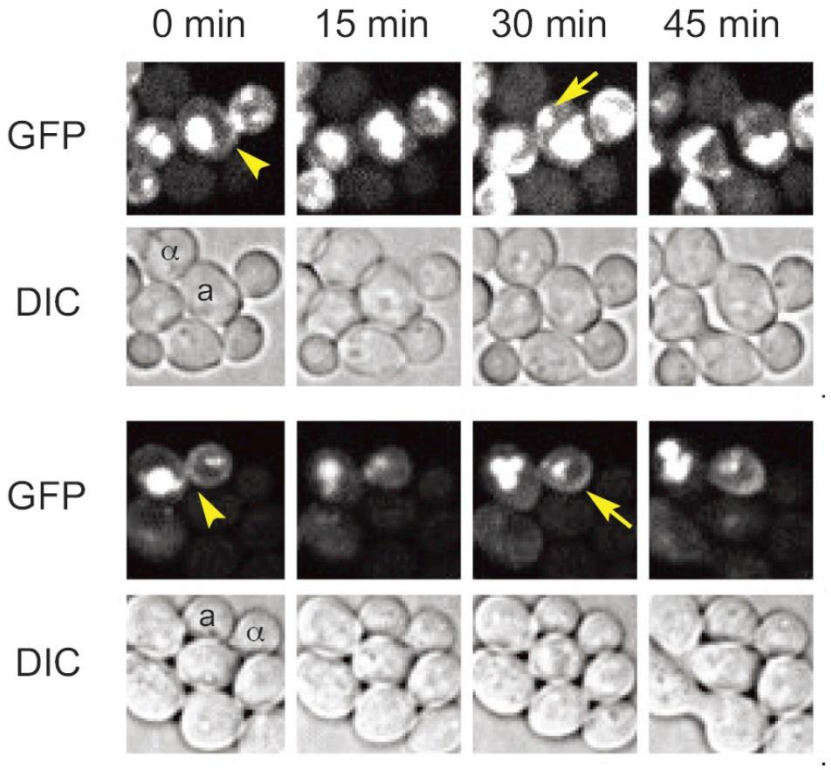

Fig. S2. Dynamic localization of the pheromone receptor as cells orient toward mating partners. *MAT***a** cells expressing an endogenously tagged receptor for the pheromone α-factor (Ste2-GFP) were mixed with *MAT*α cells and incubated at 30°C for the indicated times. Arrowheads indicate localization of the receptor to the default polarity site, whereas arrows indicate redistribution of the receptor to the chemotropic site before morphogenesis. The cell pictured in the lower rows formed a zygote with the indicated *MAT*α cell between the 60- and 75-min time points. Images are representative of two independent experiments.

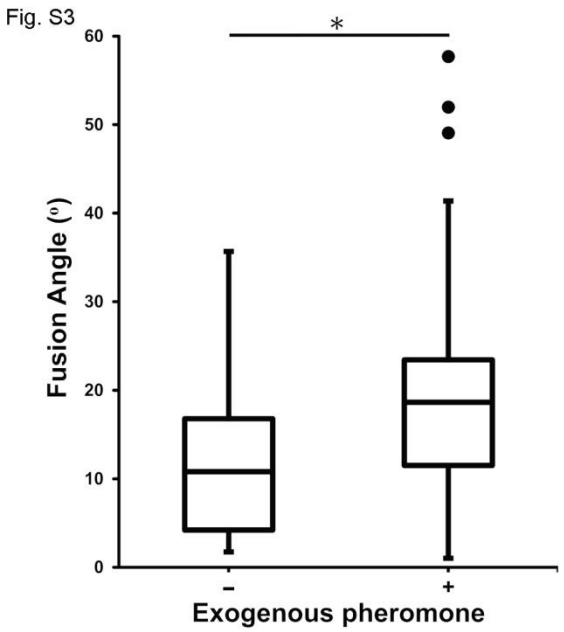

Fig. S3. Exogenous pheromone induces the formation of angled zygotes. Wild-type (WT) strains DSY257 (*MAT***a** *bar1*Δ) and DSY129 (*MAT*α *bar1*Δ) were mated for up to 4 hours on standard plate medium (-) or on medium containing 60 nM pheromone (+). Fusion angles were measured as shown in Fig. 4A. **P* = 0.0003; $n \geq 46$ cells from one experiment.

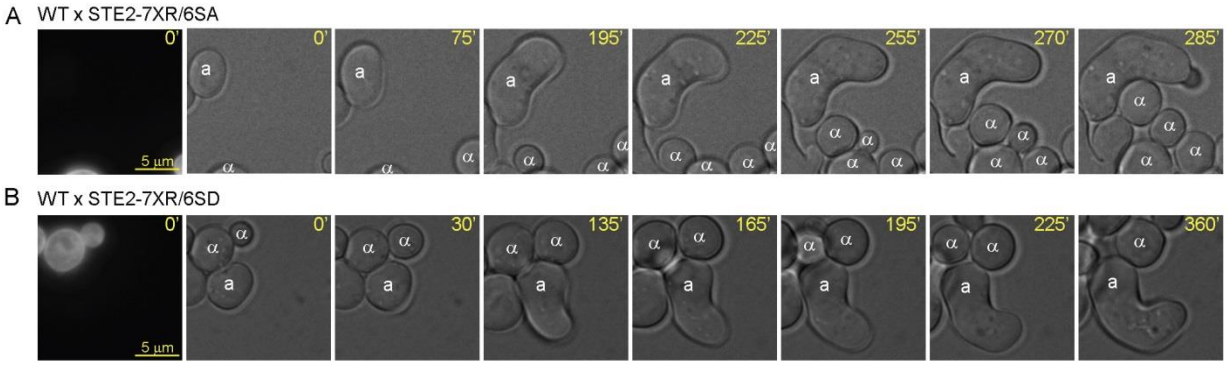

Fig. S4. Time-lapse images of elongating and turning *MAT*a *STE2*$^{7XR\ 6SA}$ and *MAT*a *STE2*$^{7XR\ 6SD}$ cells in mating mixtures. (**A** and **B**) Examples of mutant cells that were responsive to pheromone, but were apparently unable to orient in response to pheromone gradients. (A) A *MAT***a** *STE2*$^{7X\ 6SA}$ cell broadly polarized its growth away from a group of WT *MAT*α cells, persistently turning as it elongated, but it failed to mate after 270 min. (B) A *MAT***a** *STE2*$^{7X\ 6SD}$ cell broadly polarized its growth away from WT *MAT*α cells with which it was in contact, persistently turning as it elongated, but it failed to mate after 360 min. These images are in addition to those in Fig. 4 and are representative of two experiments for each mutant strain.

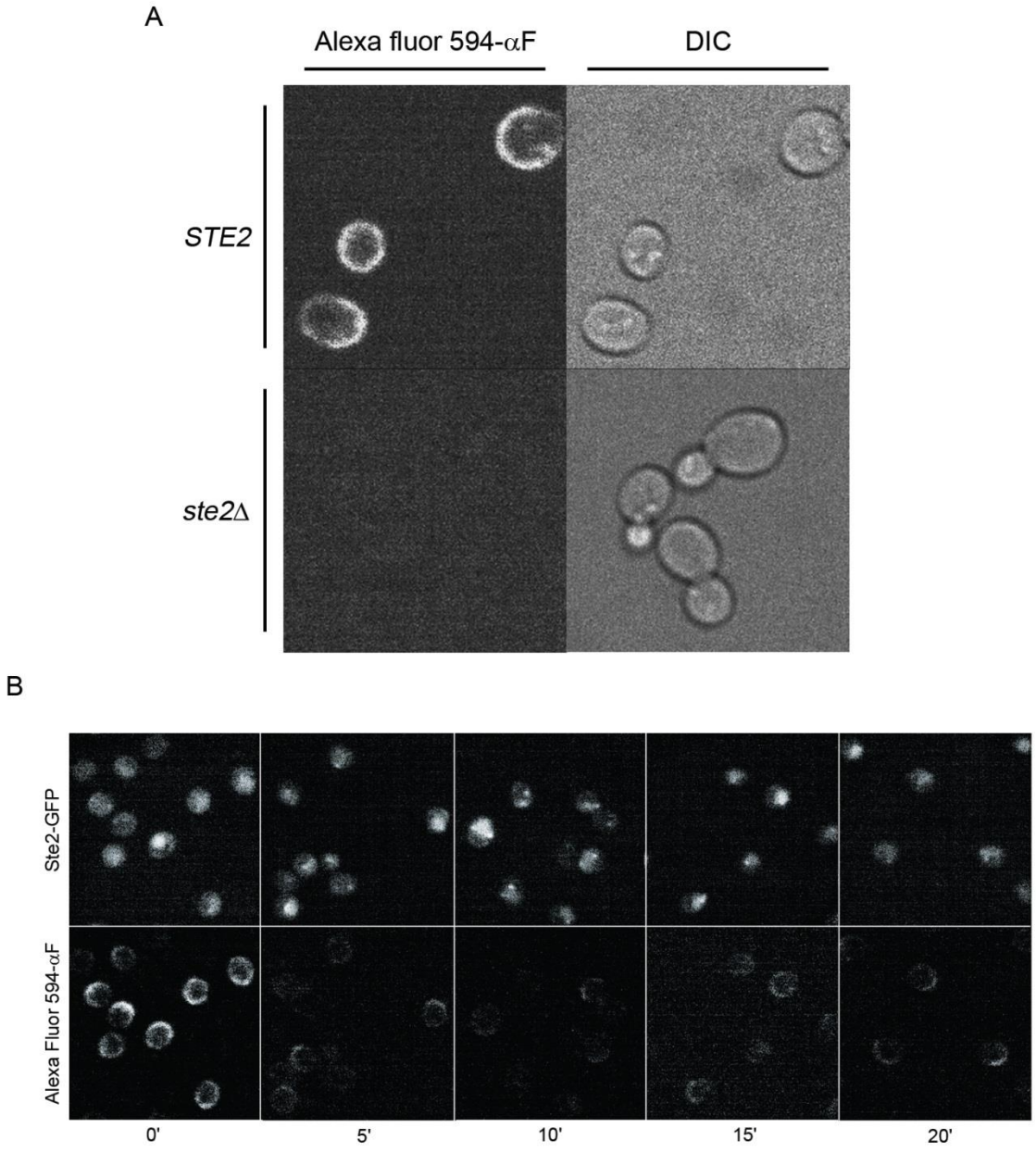

Fig. S5. Surface distribution of the pheromone receptor as assayed by Alexa Fluor 594–conjugated α-factor binding. (**A**) Alexa Fluor 594–conjugated α-factor binds specifically to the Ste2 pheromone receptor. WT (DSY257) and *ste2*Δ (EDY208) cells were stained with labeled α-factor and imaged as described in Materials and Methods. Images are representative of two experiments. (**B**) Alexa Fluor 594–conjugated α-factor reveals receptor on the surface of cells in which Ste2-GFP was undetectable. Vegetative and pheromone-stimulated cells expressing Ste2-GFP (DMY169) were treated with sodium azide at the indicated times and either imaged at 488 nm (top) or stained with Alexa Fluor 594–conjugated α-factor and imaged at 561 nm (bottom). Images are representative of two experiments.

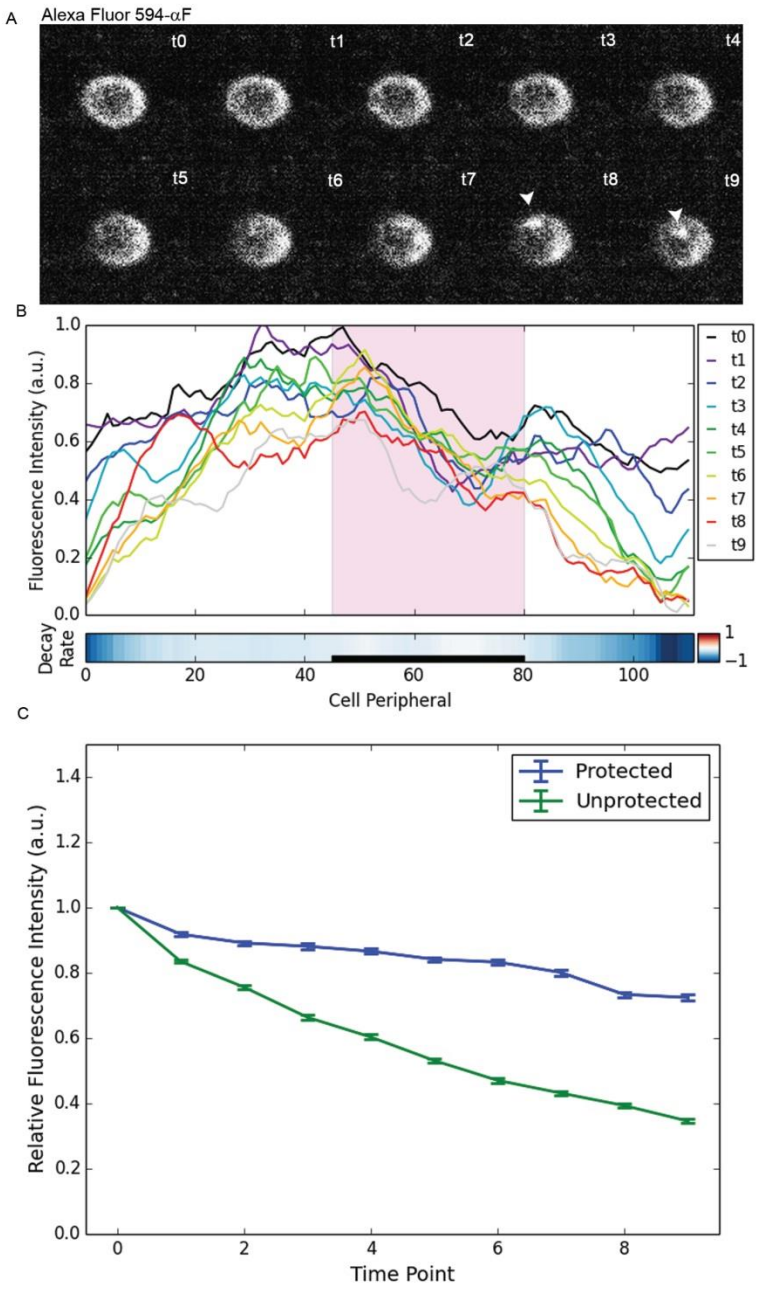

Fig. S6. Receptor internalization assay. (**A**) Time-lapse images of a cell internalizing receptors bound to Alexa Fluor 594–conjugated α-factor. The arrowheads indicate internalized label. (**B**) Line graphs showing the change in plasma membrane fluorescence over time with the high frequency noise filtered out for the cell shown in (A). The decay rate represents the change in plasma membrane fluorescence around the cell from the first to last time point, with white denoting no loss of signal and dark blue corresponding to complete loss. The pink box and black bar indicate the putative protected region. (**C**) The graph represents the average rate of plasm membrane signal decay for the front and back of cells that exhibited a discrete region of the plasma membrane with a statistically significantly slower rate of signal loss than the remainder of the plasma membrane (n = 12 cells). The area of receptor protection was defined as the points in the 30th percentile for decay rate (blue line), whereas the remainder of the plasma membrane was defined as unprotected (green line). Data are means ± SEM of three experiments.

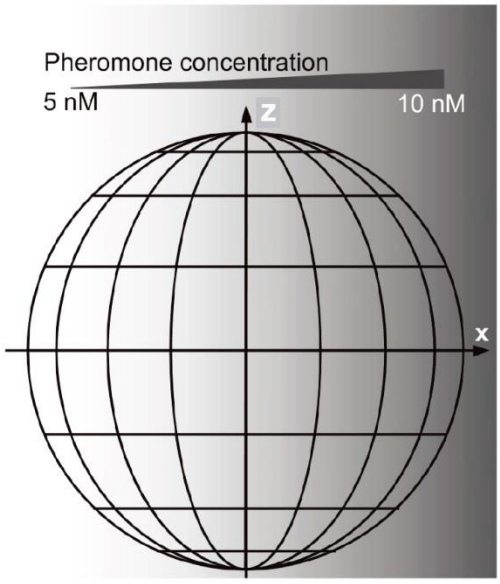

Fig. S7. Spatial model of the computational yeast cell. The cell of radius r was discretized into n latitude bands and each latitude band was cut into m patches. In this study, n = 16 and m = 40. Molecules in the "pizza slices" around the poles diffuse among the three neighboring patches; molecules in other patches diffuse among the four neighboring patches.

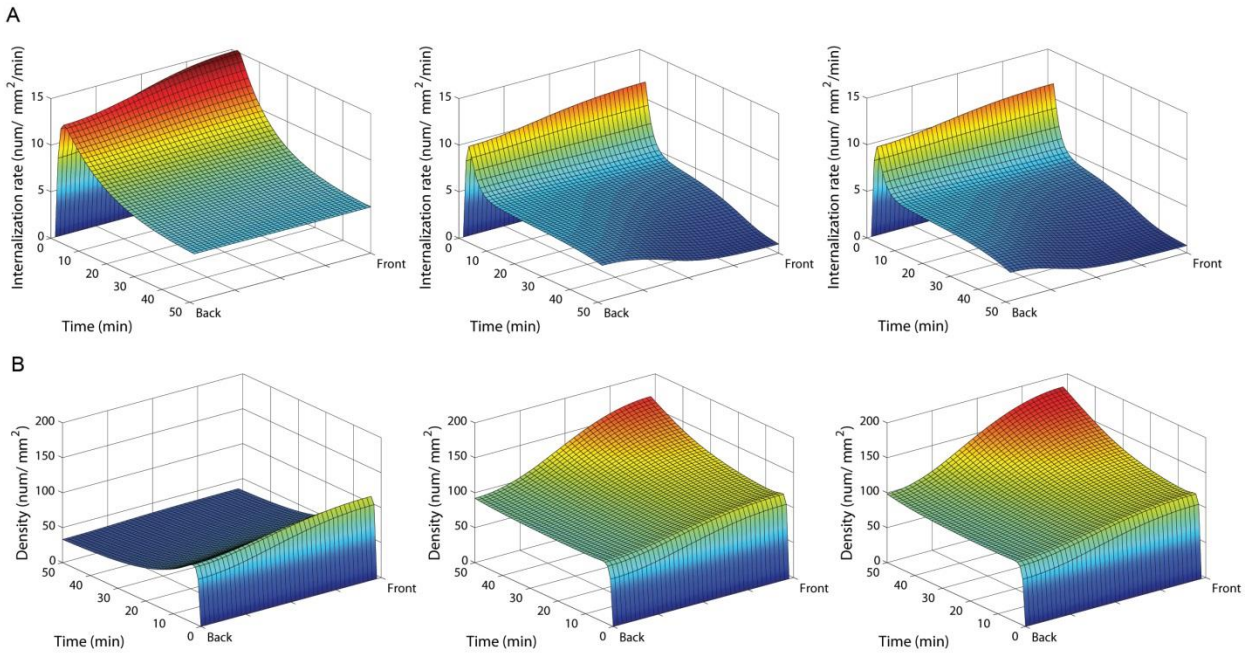

Fig. S8. Computational model of receptor dynamics. (**A** and **B**) Outputs from Networks 1 to 3 are shown from left to right. (A) Rate of receptor internalization. In Network 1, without downstream regulation, the rate of receptor internalization decreases uniformly as the number of receptors on the plasma membrane decreases. In Network 2, receptor interaction begins faster on the side of the cell facing the gradient, but this difference inverts within 15 min as $G\beta^{P}\gamma$ inhibits Yck. In Network 3, receptor internalization becomes slower on the side of the cell facing the gradient within 12 min as the Gα-dependent recruitment of Fus3 locally enhances the phosphorylation of Gβ. (B) Localization of activated receptor. The activated receptor does not polarize in Network 1, but polarizes robustly in Network 2. It polarizes to a similar degree in Network 3, but this occurs about 3 min faster than in Network 2.

Fig. S9

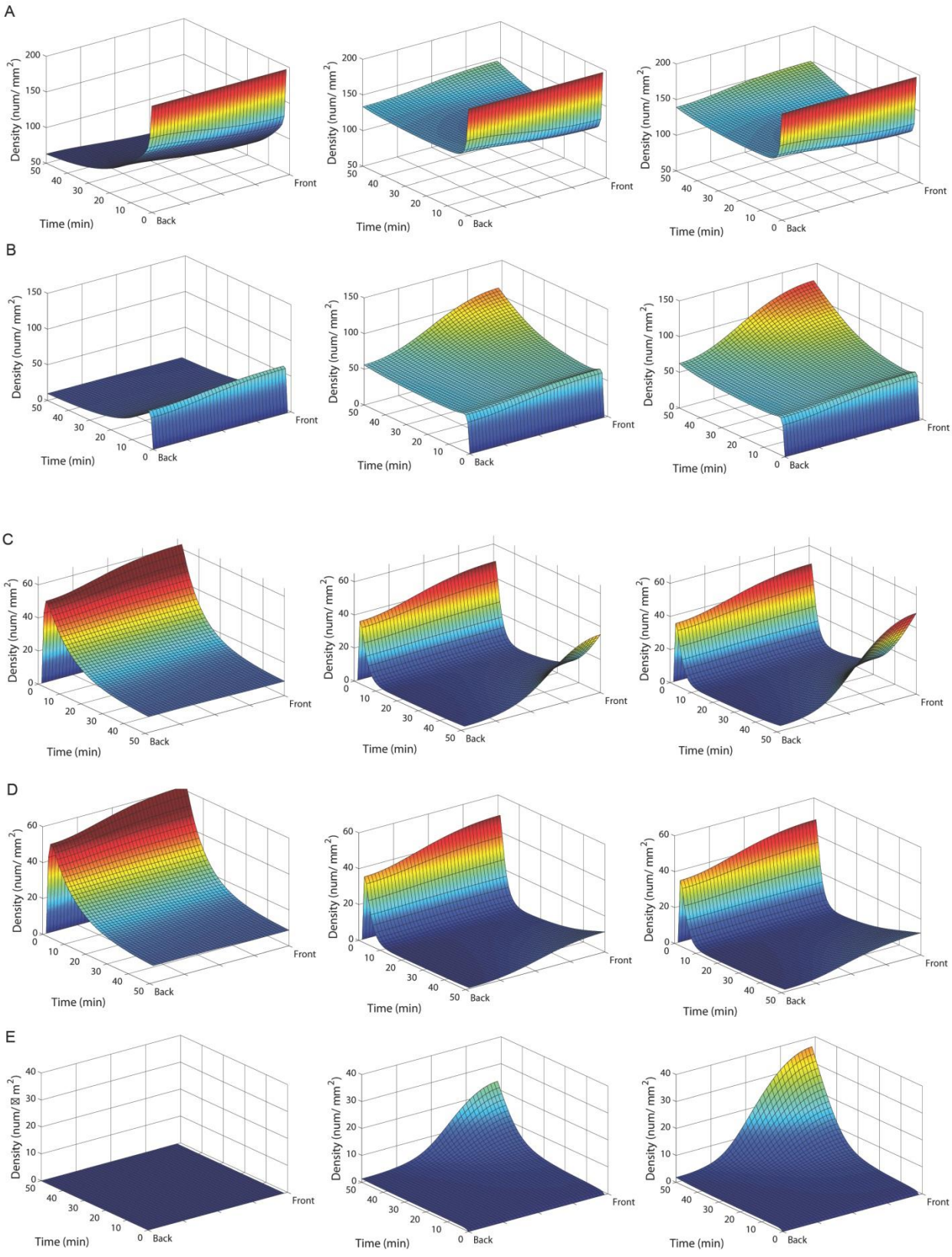

Fig. S9. Computational model of G protein dynamics. (**A** to **E**) Outputs from Networks 1 to 3 are shown from left to right. No polarity is generated in Network 1, nor does the heterotrimeric G protein polarize substantially in Networks 2 or 3; However, activated Gα steadily accumulates on the side of the cell closest to the gradient, whereas its abundance remains constant on the opposite side in these networks. In contrast, total free Gβγ undergoes a precipitous drop in abundance, partially because of the interaction of $G\beta^{P}\gamma$ with Yck, before recovering and becoming highly concentrated on the side of the cell facing the gradient. Free $G\beta^{P}\gamma$ ultimately becomes the most polarized component, reaching an abundance that is twice (Network 2) or three times (Network 3) greater than that of Gβγ in a small region of the cell surface. (A) Heterotrimeric G protein. (B) Activated Gα. (C) Total free Gβγ (unphosphorylated and phosphorylated). (D) Free Gβγ. (E) Free $G\beta^{P}\gamma$.

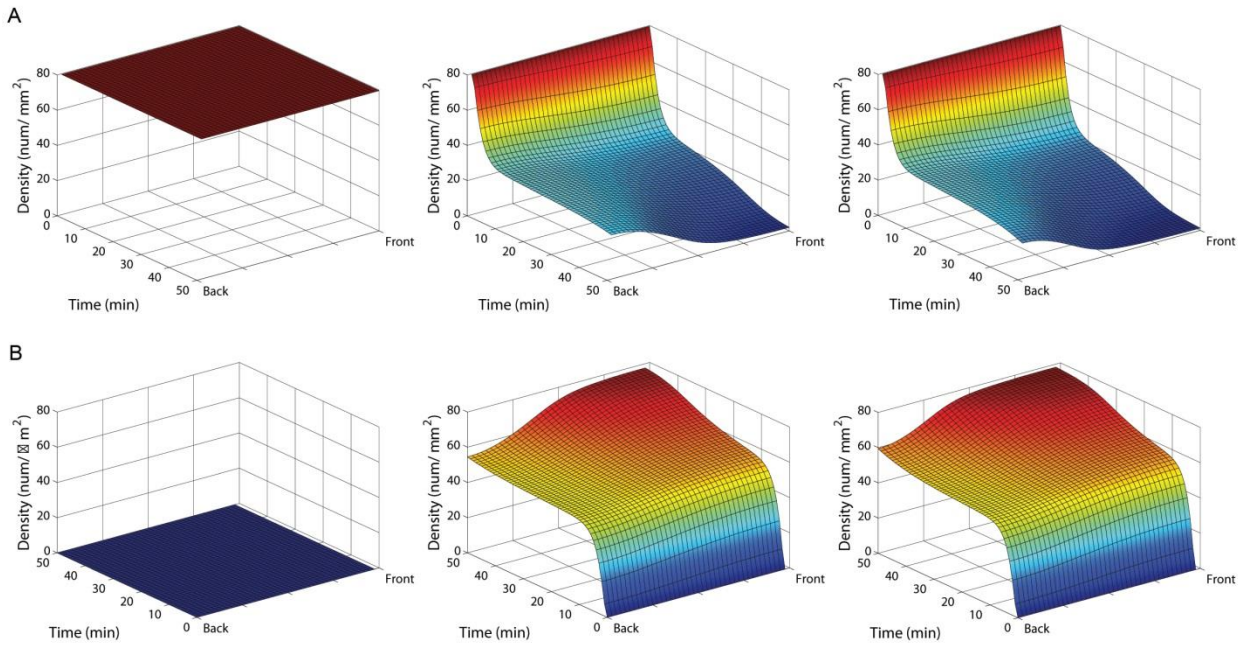

Fig. S10. Computational model of Yck dynamics. (**A** and **B**) Outputs from Networks 1 to 3 are shown from left to right. The time axes are plotted in opposite directions in (A) and (B). In Network 1, Yck is unregulated, and therefore, unaffected by the pheromone gradient. In Networks 2 and 3, free Yck concentrates to the back side of the cell, whereas Yck-G$\beta^P\gamma$ concentrates to the front side of the cell. (A) Distribution of free Yck. (B) Distribution of G$\beta^P\gamma$-bound Yck.

Table S1. Yeast strains used in this study.

Strain	Background	Genotype	Reference
DSY257	BF264-15D	*MAT***a** *bar1*Δ *ade1 his2 leu2-3,112 trp1-1a ura3*Δ	Stone lab
DMY224		*MAT***a** *his3 leu2 ura3-52 STE2-GFP::LEU2*	(*6*)
DMY222		*MAT***a** *his3 leu2 ura3-52 yck1-D1::ura3 yck2-2^{ts} STE2-GFP::LEU2*	(*6*)
AIY100	BY4741	*MAT***a** *SST2-GFP-KanMX6 ste2^{7XR}-mCherry-caURA3 Gpa1^{G302S}*-HisMX6 YCplac111	This study
AIY101	BY4741	*MAT***a** *SST2-GFP-KanMX6 ste2^{7XR}-mCherry-caURA3 gpa1^{G302S}-HisMX6* YCplac111/GAL1-Ste4	This study
AIY221	BY4741	*MAT***a** *SST2-GFP-KanMX6 ste2^{7XR}-mCherry-caURA3 gpa1^{G302S}-HisMX6* ste4$^{T320A\ S335A}$(int.)::*LEU2*	This study
AIY109	BY4741	*MAT***a** *SST2-GFP-KanMX6 ste2^{7XR}-mCherry-*	
AIY164	BY4741	*caURA3 gpa1^{G302S}-HisMX6* YCplac111/GAL1-ste4$^{T320A\ S335A}$	Deletion library strain
YDB111	BY4741	*MAT***a** *his3*Δ1 *leu2*Δ0 *met15*Δ0 *ura3*Δ0 *ste4*Δ::*KanMX4* *MAT***a** *SST2-GFP-KanMX6 ste2^{7XR}-mCherry-caURA3 gpa1^{G302S}-HisMX6*	(*22*)
DMY169	BF264-15D	*MAT***a** *bar1*Δ *ade1 his2 leu2-3,112 trp1-1a ura3*Δ *STE2-GFP::LEU2*	(*6*)

AIY197	BF264-15D	*MAT***a** *ste4$^{T320A\ S335A}$ bar1*Δ *ade1 his2 leu2-3,112 trp1-1a ura3*Δ *STE2-GFP::LEU2*	This study
RDY114	BF264-15D	*MAT***a** *ste4$^{T320A\ S335A}$ bar1*Δ *ade1 his2 leu2-3,112 trp1-1a ura3*Δ	(*21*)
DSY246	BF264-15D	*MAT*α *bar1*Δ *ade1 his2 leu2-3,112 trp1-1a ura3*Δ	Stone lab
AIY273	BF264-15D	*MAT***a** *bar1*Δ *ade1 his2 leu2-3,112 trp1-1a ura3*Δ *ste7*Δ*::KanMX* YCplac22/GAL1-Ste7 pRS416/ADH1-VF1-Yck1 pRS415/ADH1-Ste4-VF2	This study
AIY276	BF264-15D	*MAT***a** *bar1*Δ *ade1 his2 leu2-3,112 trp1-1a ura3*Δ *ste7*Δ*::KanMX* YCplac22/GAL1-Ste7 pRS416/ADH1-VF1-Yck1 pRS415/ADH1-VF2	This study
AIY275	BF264-15D	*MAT***a** *bar1*Δ *ade1 his2 leu2-3,112 trp1-1a ura3*Δ *ste7*Δ*::KanMX* YCplac22/GAL1-Ste7 pRS415/ADH1-Ste4-VF2 pRS416/ADH1-VF1	This study
RDY126	BF264-15D	*MAT***a** *ste4::URA3 GFP-STE4::ura3 bar1*Δ *ade1 his2 leu2-3,112 trp1 ura3*Δ	(*21*)
NWY069	BF264-15D	*MAT***a** *bar*Δ *ste4$^{T320A\ S335A}$* Δ*ste18::URA3 Δarg5/6::G418* Δ*lys1::hph ade1 his2 leu2-3,112 trp1-1a ura3*Δ YCplac22/GAL1-3xHA-Ste18	This study

		YCplac111/GAL1-ste4$^{T320A\ S335A}$	
NWY068	BF264-15D	*MAT***a** *bar*Δ Δ*ste18::URA3* Δ*arg5/6::G418* Δ*lys1::hph ade1 his2 leu2-3,112* *trp1-1a ura3*Δ YCplac22/GAL1-3xHA-Ste18 YCplac111/GAL1-Ste4	This study
NWY071	BF264-15D	*MAT***a** *bar*Δ Δ*ste18::URA3* Δ*arg5/6::G418* Δ*lys1::hph ade1 his2 leu2-3,112* *trp1-1a ura3*Δ YCplac22 YCplac111	This study
NWY074	BF264-15D	*MAT***a** *bar*Δ *ste4$^{T320A\ S335A}$* Δ*ste18::URA3* Δ*arg5/6::G418* Δ*lys1::hph ade1 his2 leu2-3,112 trp1-1a ura3*Δ YCplac22 YCplac111	This study
NWY073	BF264-15D	*MAT***a** *bar1*Δ *ade1 his2 leu2-3,112* *trp1-1a ura3*Δ pESC-LEU/GAL1-myc-Yck1	This study
NWY052	BF264-15D	*MAT***a** *bar1*Δ Δ*ste18::URA3* Δ*lys1::hph* *Δarg5/6::G418 ade1 his2 leu2-3,112* *trp1-1a ura3*Δ YCplac22/GAL1-His6x-Ste18 YCplac111/GAL1-Ste4	This study
EDY208	BF264-15D	*MAT***a** *bar1*Δ *ade1 his2 leu2-3,112* *trp1-1a ura3*Δ *ste2*Δ::*KanMX* #1a	Stone lab
DSY129	BF264-15D	*MAT*α *ade1 his2 leu2-3,112* *trp1-1a ura3*Δ	Stone lab
XWY005	BF264-15D	*MAT***a** *ade1 his2 leu2-3,112* *trp1-1a ura3*Δ	This study

		ste2$^{7XR\text{-}GPAAD}$::URA3	
XWY027	BF264-15D	*MAT*α *ade1 his2 leu2-3,112 trp1-1a ura3*Δ pRS406/GFP-BUD1	This study
XWY008	BF264-15D	*MAT***a** *ade1 his2 leu2-3,112 trp1-1a ura3*Δ *ste2$^{6SA\text{-}7XR\text{-}GPAAD}$::URA3*	This study
XWY018	BF264-15D	*MAT***a** *ade1 his2 leu2-3,112 trp1-1a ura3*Δ *ste2$^{6SD\text{-}7XR\text{-}GPAAD}$::URA3*	This study
AIY301	BF264-15D	*MAT***a** *bar1*Δ *ade1 his2 leu2-3,112 trp1-1a ura3*Δ *STE2-GFP::LEU2 GIC2-PBD-RFP::URA3*	This study
RDY102	BF264-15D	*MAT***a** *bar1*Δ *ade1 his2 leu2-3,112 trp1-1a ura3*Δ ste4Δ::URA3	Stone lab
XWY011	BF264-15D	*MAT***a** *bar1*Δ *ade1 his2 leu2-3,112 trp1-1a ura3*Δ YCplac111/GAL1-Ste4	This study
XWY033	BF264-15D	*MAT***a** *bar1*Δ *ade1 his2 leu2-3,112 trp1-1a ura3*Δ YCplac111/GAL1-ste4$^{T320A\ S335A}$	This study

Table S2. Plasmids used in this study.

Plasmid #	Plasmid name	Plasmid marker/type	Reference
MCB26	YCplac111/GAL1-Ste4	LEU2/CEN	(*50*)
DMB115	YCplac22-GAL1-myc-Yck1	TRP1/CEN	This study
DMB114	pESC-LEU/GAL1-myc-Yck1	LEU2/2μm	This study
RDB131	YCplac111/GAL1-ste4$^{T320A\ S335A}$	LEU2/CEN	(*21*)
NWB032	YCplac22/GAL1-3xHA-Ste18	TRP1/CEN	This study
AIB130	YIplac128/ste4$^{T320A\ S335A\ N\Delta112}$	LEU2/INT	This study
DSB155	YCplac111	LEU2/CEN	(*53*)
DSB156	YCplac33	URA3/CEN	(*53*)
DSB157	YCplac22	TRP1/CEN	(*53*)
LHP1921	Ste2$^{1-419}$-GFP	LEU2/INT	(*50*)
p416-VF1	pRS416/ADH1-Venus Fragment 1	URA3/2μm	(*54*)
p415-VF2	pRS415/ADH1-Venus Fragment 2	LEU2/2μm	(*54*)
pPC2	pRS416/ADH1-VF1-Yck1	URA3/2μm	(*61*)
AIB201	pRS415/ADH1-Ste4-VF2	LEU2/2μm	This study
MCB40	YCplac22/GAL1-His6x-Ste18	TRP1/CEN	(*50*)
	YIp211/Gic2-PBD-RFP	URA3/INT	(*52*)
DLB3850	pRS306/STE2$^{(600-1296)-7XR-GPAAD-3'UTR}$	URA3/INT	Lew lab
DLB3784	pRS306/STE2$^{(600-1296)-6SA-7XR-GPAAD-3'UTR}$	URA3/INT	Lew lab
DLB3851	pRS306/STE2$^{(600-1296)-6SD-7XR-GPAAD-3'UTR}$	URA3/INT	Lew lab
	pRS406/GFP-BUD1	URA3/INT	Arkowitz lab

Table S3. Equations used for the spatial model of the yeast cell.

Eq #	Equation	Comments
1	$h_v = \frac{\pi r}{n}$	Latitudinal patch spacing
2	$h_{ih} = r\sqrt{1 - \cos^2(\frac{2i+1}{2n}\pi)}$	Longitudinal patch spacing
3	$x_{ij} = \sqrt{r^2 - z_{ij}^2}\cos(\frac{2j+1}{2m}2\pi)$, $y_{ij} = \sqrt{r^2 - z_{ij}^2}\sin(\frac{2j+1}{2m}2\pi)$ and $z_{ij} = r\cos(\frac{2i+1}{2n}\pi)$	The position of the $\{i,j\}$-patch, (x_{ij}, y_{ij}, z_{ij})
4	$[\mathrm{L}(x_{ij})] = [\mathrm{L}(r)] + (x_{ij} - r)\cdot\psi$	Pheromone concentration of the $\{i,j\}$-patch; $\psi = 1.25nM/\mu m$
5	$D\nabla^2[S_k(i,j)] = D(\frac{[S_k(i-1,j)] + [S_k(i+1,j)] - 2[S_k(i,j)]}{h_v^2} + \frac{[S_k(i,j-1)] + [S_k(i,j+1)] - 2[S_k(i,j)]}{h_{ih}^2})$	Diffusion of the k-th molecular species Sk in the $\{i,j\}$-patch[a]
6	$D\nabla^2[S_k(1,j)] = D(\frac{[S_k(1,j)] + [S_k(3,j)] - 2[S_k(2,j)]}{h_v^2} + \frac{[S_k(1,j-1)] + [S_k(1,j+1)] - 2[S_k(1,j)]}{h_{1h}^2})$	Diffusion of the k-th molecular species Sk in the patches ringing the north pole[a]
7	$D\nabla^2[S_k(n,j)] = D(\frac{[S_k(n,j)] + [S_k(n-2,j)] - 2[S_k(n-1,j)]}{h_v^2} + \frac{[S_k(n,j-1)] + [S_k(n,j+1)] - 2[S_k(n,j)]}{h_{nh}^2})$	Diffusion of the k-th molecular species Sk in the patches ringing the south pole[a]

[a]D = 0.001 μm^2/s was used for all molecular species.

Table S4. Definitions and parameters. Parameter values are color-coded according to the network. Those in black are used in all three networks. Blue values correspond specifically to network 1, whereas those in green and red correspond to networks 2 and 3, respectively.

Parameter	Description	Initial Value	Reaction Rate [a]	Value
r	Cell radius	2μm	krs	$7.96 \times 10^{-2}\mu m^{-2}s^{-1}$ (*62*)
sa	Cell surface area	$50.27\mu m^2$	krl	$3.32 \times 10^{-3}\mu m^3 s^{-1}$ (*62*)
v	Cell volume	$33.51\mu m^3$	krlm	$0.01 s^{-1}$ (*65*)
L(r)	Pheromone at cell front	10nM	kgs	$7.96 \times 10^{-2}\mu m^{-2}s^{-1}$
L(-r)	pheromone at cell back	5nM	kga	$5.03 \times 10^{-4}\mu m^2 s^{-1}$ (*62*)
R	Inactive receptor	10,000/sa (*10*)	kgad	$0.11 s^{-1}$ (*62*)
RL	Active receptor	0	kgd	$50.3\mu m^2\ s^{-1}$ (*62*)
G	Heterotrimeric G protein	10,000/sa (*10*)	ki0	$5.03 \times 10^{-6}\mu m^2 s^{-1}$ (*62*)
Ga	Active Gα	0	ki1	$2.51 \times 10^{-5}\mu m^2 s^{-1}$ (*10*)
Gd	Inactive Gα	0	D	$0.001\mu m^2 s^{-1}$ (*63*)
Gbg	Gβγ	0	kbp0	0; $5.8 \times 10^{-3}s^{-1}$; $5.8 \times 10^{-3}s^{-1}$
GbgP	$G\beta^P\gamma$	0	kbpd	0; $1 \times 0^{-3}s^{-1}$; $1 \times 10^{-3}s^{-1}$
Yck	Yck1/2	[b]4,000/sa	kbp1	0; 0; $1 \times 10^{-5}\mu m^2 s^{-1}$
YckGbgP	Yck1/2-$G\beta^P\gamma$ complex	0	kbp2	0; 0; $1 \times 10^{-7}\mu m^4 s^{-1}$
Fus3	Inactive Fus3	[c]2,130/v	kyi	0; $5 \times 10^{-3}\mu m^2\ s^{-1}$; $5 \times 10^{-3}\ \mu m^2 s^{-1}$
Fus3P	Active Fus3	0	kya	0; $3 \times 10^{-3}\ s^{-1}$; $3 \times 10^{-3}s^{-1}$
			kfa	0; 0; [d]3 $\mu m^2 s^{-1}$
			kfd	0; 0; $1\ s^{-1}$ (*64*)

[a]Rate constants from Table S5. [b]The total number of Yck molecules per cell was reported to be 7,790 (*65*). We assumed that there were 4,000 on the cell surface. [c]The total number of Fus3 molecules per cell was reported to be 8,480 (*65*), with about 25% in the cytoplasm (*64*). [d]We set Fus3 phosphorylation to be three times faster than its dephosphorylation based on a study by Maeder *et al*. (*64*).

Table S5. Reaction formulae.

Rx #	Reaction	Comments
1	$\emptyset \xrightarrow{k_{rs}} \mathrm{R}$	Synthesis of pheromone receptor
2	$\mathrm{R} + \mathrm{L} \underset{k_{rlm}}{\overset{k_{rl}}{\rightleftharpoons}} \mathrm{RL}$	Association/disassociation of receptor & pheromone
3	$\emptyset \xrightarrow{k_{gs}} \mathrm{G}$	Synthesis of heterotrimeric G protein
4	$\mathrm{RL} + \mathrm{G} \xrightarrow{k_{ga}} \mathrm{RL} + \mathrm{Ga} + \mathrm{Gbg}$	Activation of G protein by liganded-receptor
5	$\mathrm{Ga} \xrightarrow{k_{gad}} \mathrm{Gd}$	Inactivation of Gα
6	$\mathrm{Gd} + \mathrm{Gbg} \xrightarrow{k_{gd}} \mathrm{G}$	Reassociation of Gα & Gβγ to form the heterotrimer
7	$\mathrm{Yck} + \mathrm{R} + (\mathrm{G}) \xrightarrow{k_{i0}} \mathrm{Yck}$	Yck1/2-stimulated internalization of inactive receptors and heterotrimeric G protein[a]
8	$\mathrm{Yck} + \mathrm{RL} + (\mathrm{G}) \xrightarrow{k_{i1}} \mathrm{Yck}$	Yck1/2-stimulated internalization of active receptors and heterotrimeric G protein[a]
9	$\mathrm{Gbg} \underset{k_{bpd}}{\overset{k_{bp0}}{\rightleftharpoons}} \mathrm{GbgP}$	Phosphorylation and dephosphorylation of Gβγ
10	$\mathrm{GbgP} + \mathrm{Yck} \underset{k_{ya}}{\overset{k_{yi}}{\rightleftharpoons}} \mathrm{YckGb}$	Association/disassociation of $G\beta^{P}\gamma$ and Yck1
11	$\mathrm{GbgP} + \mathrm{Fus3} \xrightarrow{k_{fa}} \mathrm{GbgP} + \mathrm{Fus3A}$	Activation of Fus3 by $G\beta^{P}\gamma$
12	$\mathrm{Fus3A} \xrightarrow{k_{fd}} \mathrm{Fus3}$	Deactivation of Fus3
13	$\mathrm{Fus3A} + \mathrm{Gbg} \xrightarrow{k_{bp1}} \mathrm{Fus3A} + \mathrm{GbgP}$	Phosphorylation of Gβ by active Fus3
14	$\mathrm{Ga} + \mathrm{Fus3A} + \mathrm{Gbg} \xrightarrow{k_{bp2}} \mathrm{Ga} + \mathrm{Fus3A} + \mathrm{GbgP}$	Gα recruitment of active Fus3 to phosphorylate Gβ

[a]The stoichiometry of the internalized receptor and heterotrimeric G protein is assumed to be 1:1.

Table S6. Partial differential equations.

Eq #	Equation
1	$\frac{\partial[\mathrm{R}]}{\partial t} = D\nabla^2[\mathrm{R}] + k_{rs} - k_{rl}[\mathrm{R}][\mathrm{L}] + k_{rlm}[\mathrm{RL}] - k_{i0}[\mathrm{Yck}][\mathrm{R}]$
2	$\frac{\partial[\mathrm{RL}]}{\partial t} = D\nabla^2[\mathrm{RL}] + k_{rl}[\mathrm{R}][\mathrm{L}] - k_{rlm}[\mathrm{RL}] - k_{i1}[\mathrm{Yck}][\mathrm{RL}]$
3	$gr0 = \min(1, [G]/[R])$
4	$gr1 = \min(1, [G]/[RL])$
5	$\frac{\partial[\mathrm{G}]}{\partial t} = D\nabla^2[\mathrm{G}] + k_{gs} + k_{gd}[\mathrm{Gd}][\mathrm{Gbg}] - k_{ga}[\mathrm{G}][\mathrm{RL}] - k_{i0} \cdot gr0[\mathrm{Yck}][R] - k_{i1} \cdot gr1[\mathrm{Yck}][\mathrm{RL}]$
6	$\frac{\partial[\mathrm{Ga}]}{\partial t} = D\nabla^2[\mathrm{Ga}] + k_{ga}[\mathrm{G}][\mathrm{RL}] - k_{gad}[\mathrm{Ga}]$
7	$\frac{\partial[\mathrm{Gd}]}{\partial t} = D\nabla^2[\mathrm{Gd}] + k_{gad}[\mathrm{Ga}] - k_{gd}[\mathrm{Gd}][\mathrm{Gbg}]$
8	$\frac{\partial[\mathrm{Gbg}]}{\partial t} = D\nabla^2[\mathrm{Gbg}] + k_{ga}[\mathrm{G}][\mathrm{RL}] - k_{gd}[\mathrm{Gd}][\mathrm{Gbg}] + k_{bpd}[\mathrm{GbgP}] - k_{bp0}[\mathrm{Gbg}] - k_{bp1}[\mathrm{Fus3A}][\mathrm{Gbg}] - k_{bp2}[\mathrm{Ga}][\mathrm{Fus3A}][\mathrm{Gbg}]$
9	$\frac{\partial[\mathrm{GbgP}]}{\partial t} = D\nabla^2[\mathrm{GbgP}] - k_{bpd}[\mathrm{GbgP}] + k_{bp0}[\mathrm{Gbg}] + k_{bp1}[\mathrm{Fus3A}][\mathrm{Gbg}] + k_{bp2}[\mathrm{Ga}][\mathrm{Fus3A}][\mathrm{Gbg}] - k_{yi}[\mathrm{Yck}][\mathrm{GbgP}] + k_{ya}[\mathrm{YckGbgP}]$
10	$\frac{\partial[\mathrm{Yck}]}{\partial t} = D\nabla^2[\mathrm{Yck}] - k_{yi}[\mathrm{Yck}][\mathrm{GbgP}] + k_{ya}[\mathrm{YckGbgP}]$
11	$\frac{\partial[\mathrm{YckGbgP}]}{\partial t} = D\nabla^2[\mathrm{YckGbgP}] + k_{yi}[\mathrm{Yck}][\mathrm{GbgP}] - k_{ya}[\mathrm{YckGbgP}]$
12	$\frac{\partial[\mathrm{Fus3}]}{\partial t} = D\nabla^2[\mathrm{Fus3}] + k_{fd}[\mathrm{Fus3A}] - k_{fa}[\mathrm{GbgP}][\mathrm{Fus3}]$
13	$\frac{\partial[\mathrm{Fus3A}]}{\partial t} = D\nabla^2[\mathrm{Fus3A}] - k_{fd}[\mathrm{Fus3A}] + k_{fa}[\mathrm{GbgP}][\mathrm{Fus3}]$